

Efficient Water Oxidation Kinetics and Enhanced Electron Transport in Li-doped TiO₂ Nanotubes Photoanodes

Lok-kun Tsui^{a,1}, Yin Xu,^{a,1} Damian Dawidowski^b, David Cafiso^b, Giovanni Zangari^{a,*}

^aDepartment of Materials Science and Engineering and CESE, University of Virginia, 395 McCormick Rd, Charlottesville, VA, 22904, USA

^bDepartment of Chemistry, University of Virginia, McCormick Road, P.O. Box 400319, Charlottesville, VA, 22904, USA

¹ these two authors contributed equally to the work

Supporting Information

I. Surface SEM image of TiO₂ nanotubes

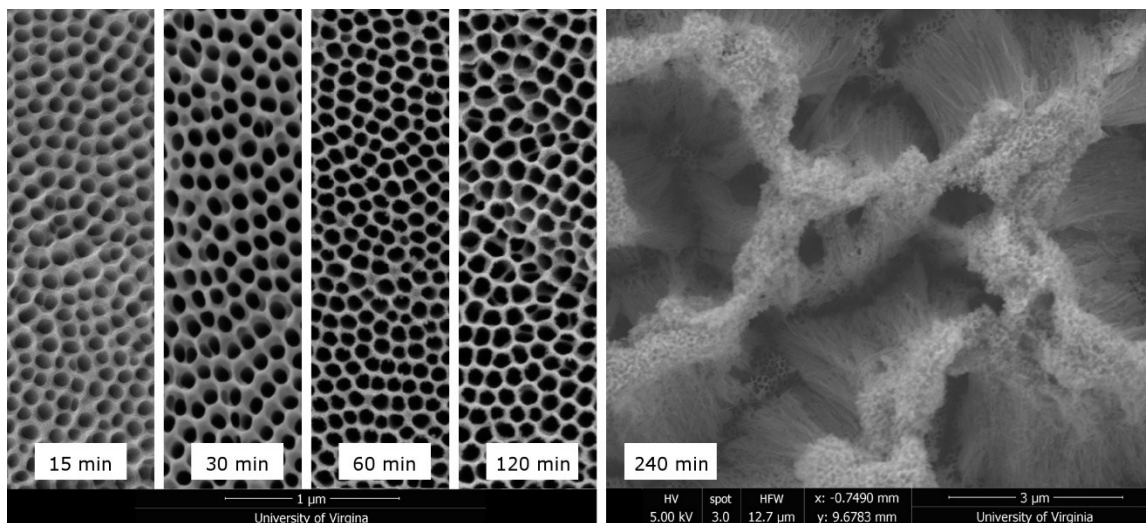


Figure S1. Surface SEM images of TiO₂ nanotubes grown for varying amounts of time. Well-ordered pores with increasing pore diameter are formed until 240 minutes where the top part collapses.

II. Pore size distribution of TiO₂ nanotubes anodized for different times

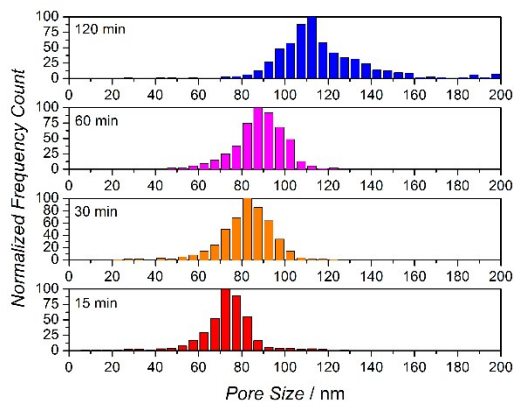


Figure S2. Pore size distribution for TiO₂ nanotubes showing an increase in the average pore size as anodization time increases.

III. Raman Spectra of $\text{Co}_3\text{O}_4/\text{CoOOH}$ modified TiO_2 NTs.

Reference Raman signals:

- Anatase TiO_2 :^[1] 144, 196, 400, 517, and 641 cm^{-1}
- Co_3O_4 :^[2,3] 197, 485, 620, and 691 cm^{-1}
- CoOOH :^[2,3] 620 and 505 cm^{-1}

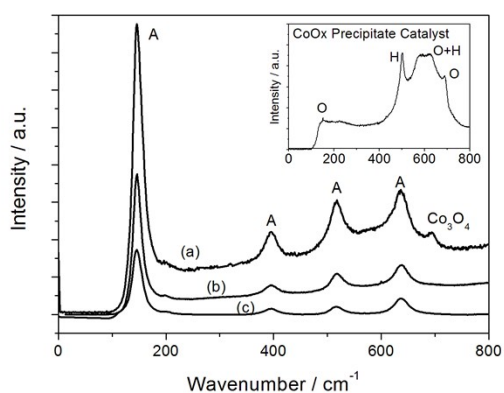


Figure S3. Raman spectra of TiO_2 nanotubes modified by (a) electrodeposited Co oxide, (b) precipitated Co oxide, and (c) photodeposited Co-Pi. Inset: Raman spectra of the precipitate extracted from the solution used to prepare (b). Key: A – anatase TiO_2 . Inset O – Co_3O_4 . Inset H – CoOOH .

IV. EDS spectra and surface mapping of CoO_x modified TiO_2 nanotubes

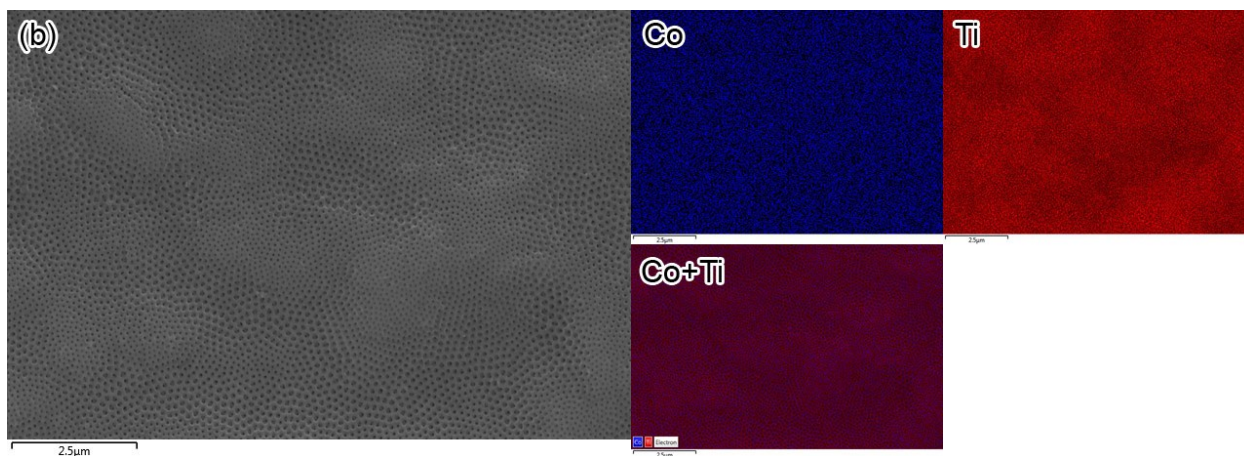
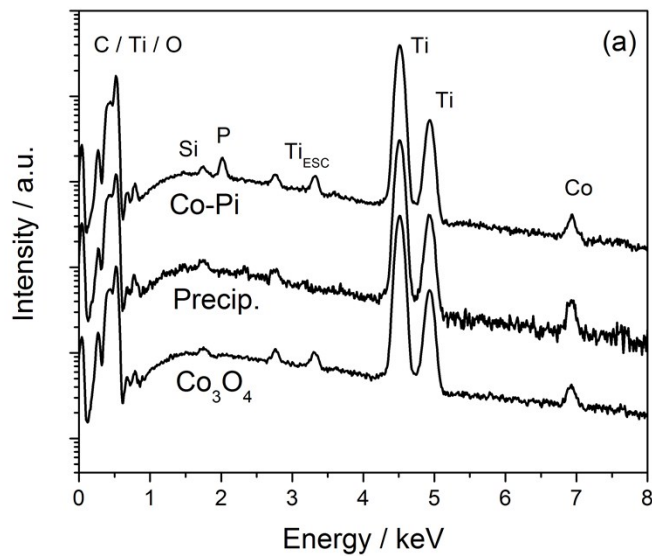


Figure S4. (a) EDS spectra of CoO_x modified TiO_2 nanotubes confirm the presence of elements Co in all three catalysts investigated and the addition of P with Co-Pi. EDS spectra are shown for the highest quantity of catalyst loading. Si originates from the carbon tape used to secure the sample. (b) EDS surface mapping of TiO_2 nanotubes modified by precipitated CoO_x catalysts shows a uniform coverage of the nanotube arrays, but no visible deposit.

V. Scanning electron microscopy studies of catalyst modified Li-TiO₂ nanotubes.

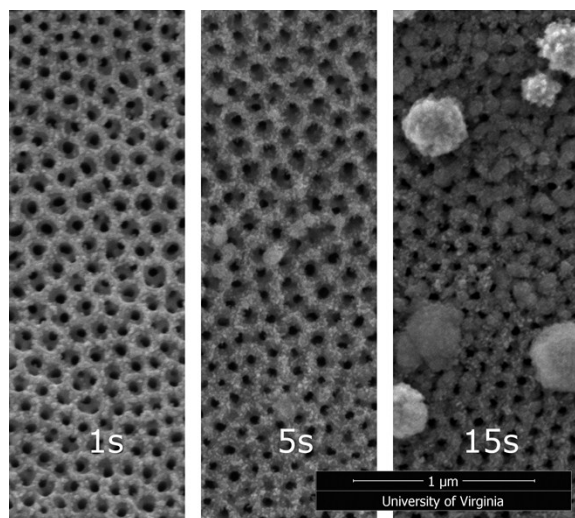


Figure S5. The morphology of electrodeposited Co oxide catalyst prepared by electrodeposition of metallic Co and then electrochemical cycling in an alkaline electrolyte changes from decoration at the mouths of the tubes to the formation of particles on the surface of the nanotube array.

VI. Photocurrent as a function of catalyst deposition amount for Co-Ox based catalysts on TiO₂ nanotubes.

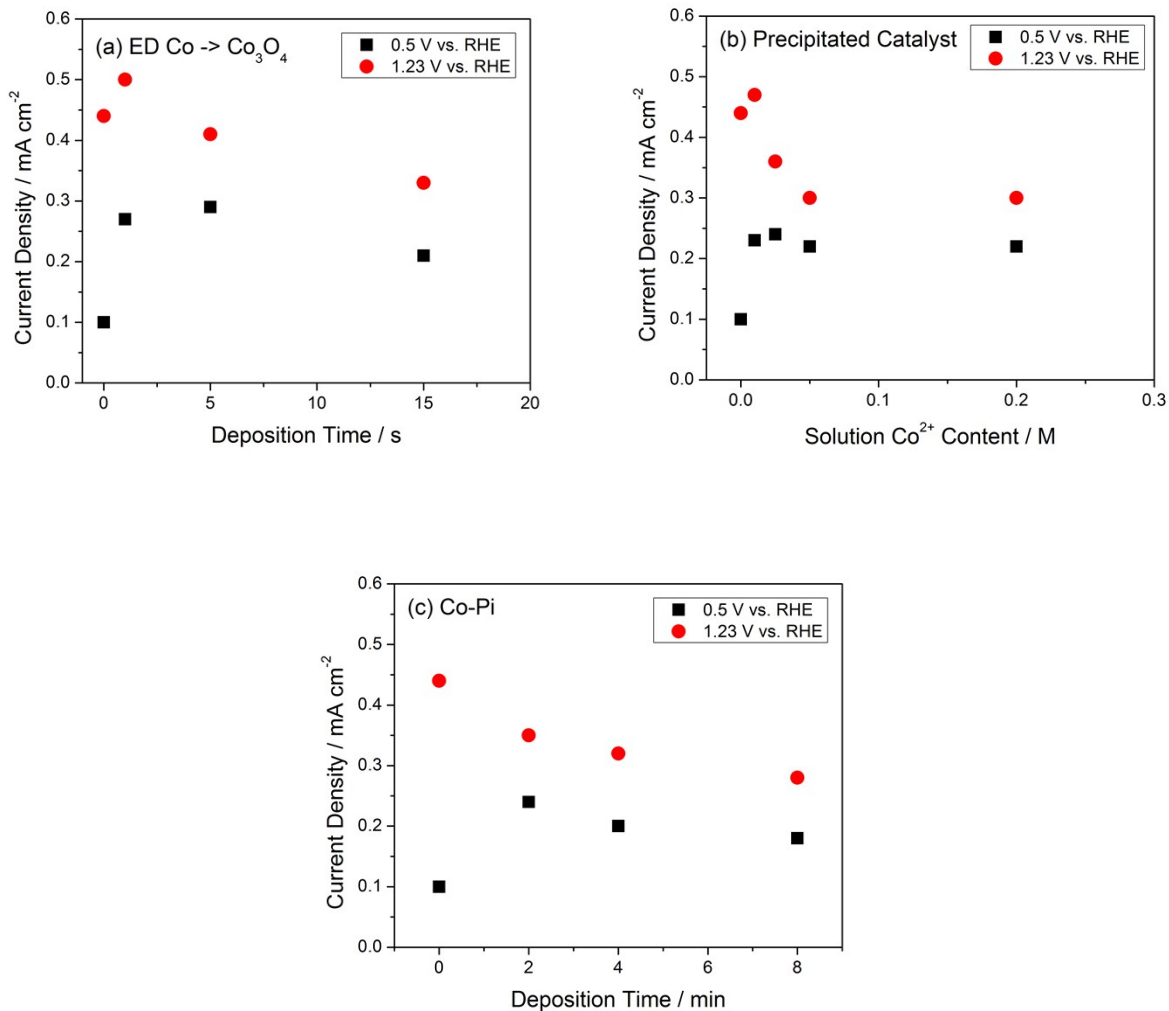


Figure S6. Photocurrent under two applied potentials for three different Co-based catalysts on TiO₂ nanotubes. Under a weak applied potential at 0.5 V_{RHE}, a twofold enhancement in the photocurrent is observed. However, at strong applied potential, adding more catalyst results in decreasing photocurrent.

VII. Charge increase for TiO₂ nanotubes with various lengths in the process of Li intercalation.

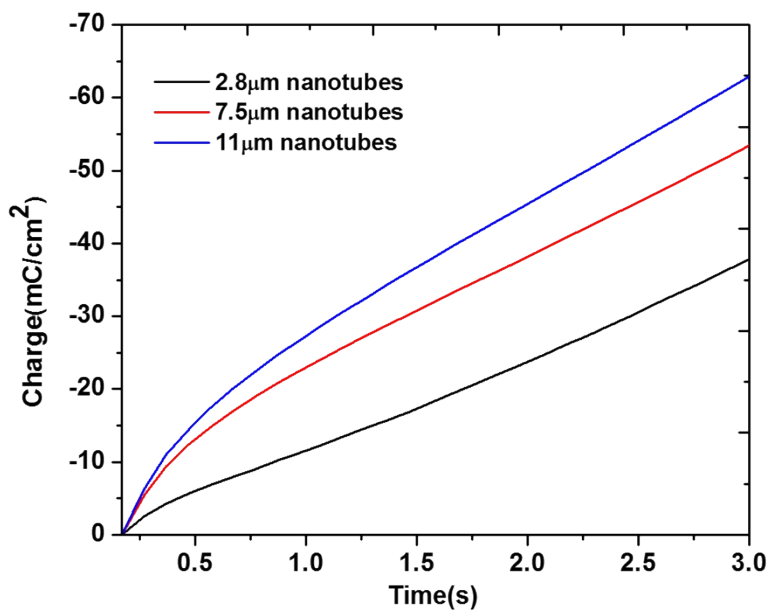


Figure S7. Charge-time curve in the process of Li-intercalation. According to Faraday's law of electrochemistry, the charge passed is proportional to the mass induced. Apparently, Li amount is increasing with the thickness of the TiO₂ layer, but not proportionally to the tube length, probably due to diffusion limitations. Furthermore, the extent of Li intercalation cannot be precisely determined due to the simultaneous occurrence of hydrogen evolution.

References

- [1] N.-G. Park, G. Schlichthörl, J. van de Lagemaat, H. M. Cheong, A. Mascarenhas, A. J. Frank, *J. Phys. Chem. B* **1999**, *103*, 3308.
- [2] B. S. Yeo, A. T. Bell, *J. Amer. Chem. Soc.* **2011**, *133*, 5587.
- [3] Y. Liu, J. A. Koza, J. a. Switzer, *Electrochim. Acta* **2014**, *140*, 359.